# Tumor-derived endothelial cells exhibit aberrant Rho-mediated mechanosensing and abnormal angiogenesis *in vitro*

**Kaustabh Ghosh, Charles K. Thodeti, Andrew C. Dudley, Akiko Mammoto, Michael Klagsbrun, and Donald E. Ingber***

Vascular Biology Program, Departments of Pathology and Surgery, Children's Hospital and Harvard Medical School, Boston, MA 02115

Edited by Robert Langer, Massachusetts Institute of Technology, Cambridge, MA, and approved May 13, 2008 (received for review January 27, 2008)

**Tumor blood vessels exhibit abnormal structure and function that cause disturbed blood flow and high interstitial pressure, which impair delivery of anti-cancer agents. Past efforts to normalize the tumor vasculature have focused on inhibition of soluble angiogenic factors, such as VEGF; however, capillary endothelial (CE) cell growth and differentiation during angiogenesis are also influenced by mechanical forces conveyed by the extracellular matrix (ECM). Here, we explored the possibility that tumor CE cells form abnormal vessels because they lose their ability to sense and respond to these physical cues. These studies reveal that, in contrast to normal CE cells, tumor-derived CE cells fail to reorient their actin cytoskeleton when exposed to uniaxial cyclic strain, exhibit distinct shape sensitivity to variations in ECM elasticity, exert greater traction force, and display an enhanced ability to retract flexible ECM substrates and reorganize into tubular networks *in vitro*. These behaviors correlate with a constitutively high level of baseline activity of the small GTPase Rho and its downstream effector, Rho-associated kinase (ROCK). Moreover, decreasing Rho-mediated tension by using the ROCK inhibitor, Y27632, can reprogram the tumor CE cells so that they normalize their reorientation response to uniaxial cyclic strain and their ability to form tubular networks on ECM gels. Abnormal Rho-mediated sensing of mechanical cues in the tumor microenvironment may therefore contribute to the aberrant behaviors of tumor CE cells that result in the development of structural abnormalities in the cancer microvasculature.**

capillary | contractility | elasticity | GTPase | mechanotransduction

Solid cancers must induce angiogenesis, the formation of new blood vessels, to promote their growth and metastasis. However, unlike normal vasculature, tumor vessels are irregularly shaped and highly tortuous, and they lack uniform pericyte and basement membrane coverage (1, 2). These structural changes contribute to vascular hyperpermeability, nonuniform blood flow and distribution, and high interstitial pressure, which together limit the effectiveness of anti-cancer chemotherapies and radiation therapies by impairing the delivery of drugs and oxygen to the tumor site (3). Normalization of the tumor vasculature that restores normal blood flow and permeability can improve cancer therapy (4). Past attempts to understand the abnormal properties of tumor vessels or normalize their structure have focused on vascular endothelial growth factor-A (VEGF-A) (5, 6), a ubiquitious tumor angiogenic factor that, alone, is capable of inducing structural and functional defects in normal blood vessels (7). However, anti-VEGF treatments only produce short-term normalization effects (8). Thus, a deeper understanding of the mechanisms responsible for the formation of abnormal tumor vasculature is required to achieve future therapeutic success.

Although angiogenic factors, such as VEGF, stimulate vascular development, capillary endothelial (CE) cell sensitivity to these factors and resulting capillary growth and pattern formation are governed by a mechanical force balance that is established by CE cells when they exert traction forces on their adhesions to extracellular matrix (ECM), which is generally stiffer than the cell (9–13). Whereas contractile forces generated in the cytoskeleton maintain the ECM in a prestressed state of isometric tension (14), changes in ECM compliance or cell distortion can feed back to modulate cell tension, and thus, the cell and its local ECM comprise an adaptive feedback system (15, 16). Any local variation in this cell–ECM force equilibrium occurring in the cellular microenvironment may produce cell shape-mediated differentials in cell growth and motility that, when repeated over space and time, can produce branching tubular networks as seen during normal vascular morphogenesis (17).

In contrast to normal CE cells, tumor-derived CE cells encounter an abnormal mechanical microenvironment and a highly heterogeneous ECM. Tumor stroma is stiffer than normal ECM, likely due to high interstitial pressure, increased fibrillar collagen deposition in capsular regions, and physical stress from the expanding solid tumor mass (18). Leakage of fibrinogen and other plasma proteins produces an extravascular cross-linked fibrin scaffold, which may also contribute to the stiff fibrotic tumor stroma (1, 19). In addition, tumor vessels often exhibit nonuniform basement membrane and pericyte coverage that may compound the mechanical and structural heterogeneity experienced by tumor CE cells (2). Turbulent blood flow in tortuous tumor vessels will likely cause abnormal vessel wall stretching as well, exposing tumor CE cells to erratic cyclic strain (20). These anomalous physical cues continuously and unpredictably alter the cell–ECM force balance that can modify tumor CE cell behavior through force-sensing integrin receptors, which transduce mechanical signals into changes in intracellular biochemistry and gene expression (21, 22).

Thus, in the present study, we asked whether the abnormal structure, form, and function of cancer vessels result from deregulation of the normal mechanosensing mechanism in tumor CE cells. By comparing the ability of CE cells isolated from normal versus tumor microvasculature to sense and respond to physical cues in their ECM, we show that tumor CE cells exhibit different sensitivities to various mechanical cues *in vitro* and that these abnormal responses, which may be implicated in the loss of normal structure in the tumor microvasculature, are due to aberrant Rho signaling.

## Results

**Tumor CE Cells Respond Abnormally to Applied Cyclic Strain.** Normal endothelial cells sense and respond to applied uniaxial cyclic

Author contributions: K.G., C.K.T., and D.E.I. designed research; K.G. and C.K.T. performed research; A.C.D., A.M., and M.K. contributed new reagents/analytic tools; K.G., C.K.T., and D.E.I. analyzed data; and K.G. wrote the paper.

The authors declare no conflict of interest.

This article is a PNAS Direct Submission.

*To whom correspondence should be addressed at: KFRL 11.127, Vascular Biology Program, Departments of Pathology and Surgery, Children's Hospital, Boston, MA 02115. E-mail: donald.ingber@childrens.harvard.edu.

This article contains supporting information online at www.pnas.org/cgi/content/full/0800835105/DCSupplemental.

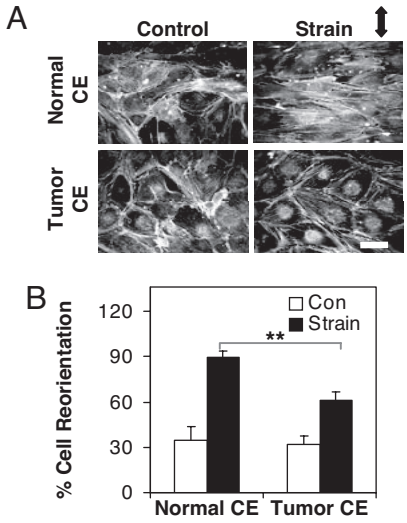


**Fig. 1.** Tumor CE cells reorient abnormally in response to uniaxial cyclic strain. (*A*) Fluorescent micrographs of normal (MDCE) and tumor CE cells cultured on FN-coated flexible silicone substrates and subjected to either no strain (Control) or 10% uniaxial cyclic strain (Strain) for 18 h at 1 Hz; arrow indicates the direction of applied strain. Actin stress fibers and nuclei were visualized by staining with Alexa4 Fluor 88-phalloidin and DAPI, respectively. (*B*) Computerized morphometric quantitation of the reorientation response in cells cultured in the absence (Control, white bars) or presence of 10% uniaxial cyclic strain (Strain, black bars). Data are presented as the percentage cells that reoriented 90° ± 30° relative to the direction of applied strain (**, $P < 0.001$). (Scale bar, 50 $\mu$m.)

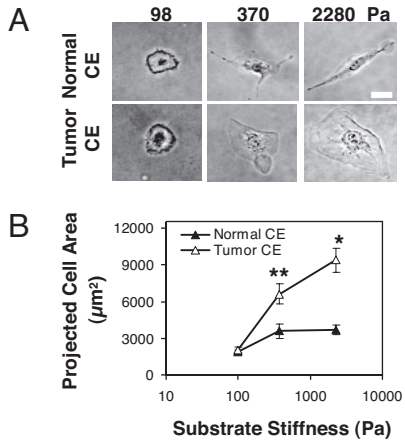


**Fig. 2.** Tumor CE cells respond abnormally to variations in ECM elasticity. (*A*) Phase contrast micrographs showing normal and tumor CE cell spreading after 6 h of culture on compliant transglutaminase-cross-linked gelatin hydrogels of varying stiffness (98, 370, or 2,280 Pa). (*B*) Average projected cell areas measured for cells cultured as described in *A* (*, $P < 0.05$; ** $P < 0.001$; each sample was compared with its immediately preceding data point). (Scale bar, 100 $\mu$m.)

strain by reorienting their actin cytoskeleton perpendicular to the direction of strain (23). To determine whether tumor CE cells exhibit normal sensitivity to mechanical cues, we subjected these cells to 10% uniaxial cyclic strain (1 Hz) and compared their reorientation response to those of three different types of nontumor CE cells. Consistent with published results obtained with various types of normal microvascular and macrovascular endothelial cells (23, 24), normal mouse dermal CE cells (MDCE; Fig. 1*A*), human dermal CE cells [HDCE; supporting information (SI) Fig. S1], and cells of the established MS1-CE cell line all reoriented their main axis and realigned their actin stress fibers perpendicular to the direction of applied strain. In contrast, CE cells isolated from TRAMP tumors failed to reorient optimally (Fig. 1*A*): Whereas ≈90% of all three nontumor CE cells reoriented perpendicular to strain direction, only 60% of tumor CE cells exhibited this response (Fig. 1*B*; $P < 0.001$). Tumor and normal CE cells displayed a similar level and distribution of VE-cadherin (Fig. S2). Thus, these differences in strain-induced reorientation do not appear to arise from differential cell–cell adhesions.

**Tumor CE Cells Exhibit Abnormal Sensitivity to Substrate Elasticity.** Variations in ECM elasticity can significantly influence cell form and function by modulating cell shape, which varies depending on the ability of the ECM to resist cell traction forces generated in the cytoskeleton; thus, cell spreading is an indirect measure of how efficiently cells sense and respond to ECM elasticity (25). Normal and tumor CE cells were cultured for 6 h on gelatin gels that varied in mechanical compliance (elasticity) from 98 to 2,280 Pa. Normal CE cells elongated (Fig. 2*A*) and increased their degree of spreading (projected cell areas) with increasing gel stiffness. They spread over 1,800 ± 200 $\mu$m$^2$ on the softest (98 Pa) gel and extended to cover approximately twice this area on gels with intermediate (370 Pa) and maximal (2,280 Pa) rigidity (Fig. 2*B*). In contrast, although tumor CE cells exhibited a similar size and shape on the most flexible ECM substrate, they spread to a much greater degree (3- to 5-fold higher) and displayed more polygonal forms on the stiffer ECM gels (Fig. 2 *A* and *B*). Moreover, whereas normal CE cells exhibited optimal spreading on the intermediate stiffness ECM, tumor CE cells continued to increase their size even on the most rigid gel (Fig. 2*B*). Thus, compared with their normal counterparts, tumor CE cells exhibit an enhanced ability to spread given the same ECM elasticity, and they require stiffer substrates to achieve maximal shape stability.

**Tumor CE Cells More Readily Form Capillary Networks *in Vitro*.** To determine whether the altered mechanosensitivity of tumor CE cells influences their ability to form capillary networks, we analyzed normal and tumor CE cells by using a fibrin gel-based *in vitro* angiogenesis assay. Fibrin was used in these studies because it represents a physiological ECM that supports both normal and tumor angiogenesis *in vivo* (26). Interestingly, at a low plating density ($2 \times 10^4$ cells per well), tumor CE cells reorganized into a robust multicellular capillary network within 24 h, whereas normal CE cells only exhibited a flattened morphology (Fig. 3*A*). Previous studies have shown that capillary formation can be enhanced *in vitro* by plating CE cells at a high density to augment the total level of cell-generated tension within the monolayer (10). Consistent with these findings, increasing the plating density of normal CE cells to $8 \times 10^4$ cells (per well) promoted capillary tube formation (Fig. 3*A*). In contrast, a similar increase in plating density caused the tumor CE cells to undergo multicellular retraction that led to gradual disruption of the tubular network, eventually resulting in the formation of large cell clumps at the highest cell plating density (Fig. 3*A*). Importantly, tumor CE cells cultured within (rather than on top of) Matrigel formed tubular structures that were abnormally dilated and nonuniform, an abnormal morphology reminiscent of that observed within the cancer microvasculature *in vivo* (Fig. 3*B*), and those cultured in fibrin gels formed large cell clumps (Fig. S3). However, normal CE cells reorganized into tubular structures of relatively uniform size under similar culture conditions (Fig. 3*B* and Fig. S3).

**Tumor CE Cells Exert Stronger Rho-mediated Traction on Their ECM Adhesions.** The findings described above suggest that tumor CE cells may respond differently to ECM mechanical cues because

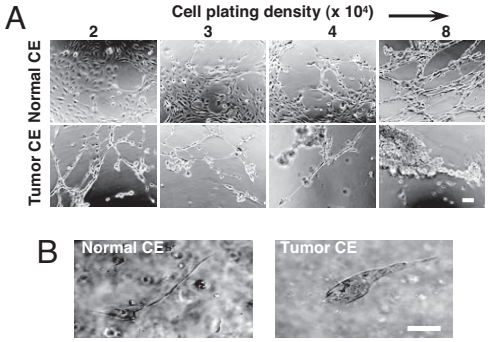


**Fig. 3.** Normal and tumor CE cells exhibit distinct angiogenic capabilities *in vitro*. Phase contrast micrographs showing normal and tumor CE cells plated either on the surface of 3D fibrin gels at the indicated plating densities and cultured for 18 h (*A*) or within 3D Matrigel at $5 \times 10^6$ cells per milliliter and cultured for 2 wk (*B*). (Scale bar, 100 $\mu$m.)

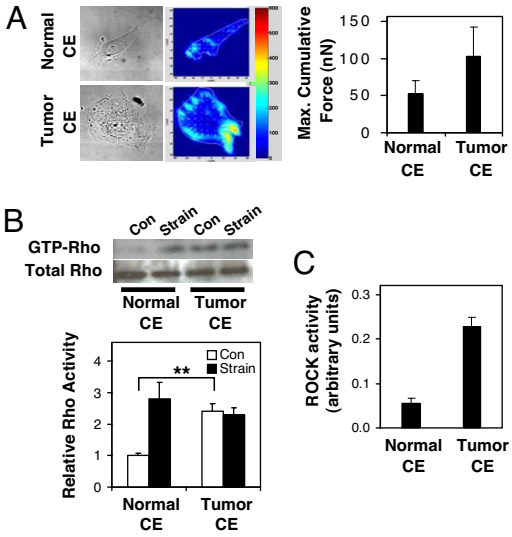


**Fig. 4.** Tumor CE cells exert stronger Rho/ROCK-mediated traction. (*A*) Traction force microscopy results showing that tumor CE cells are more contractile than normal CE cells. (*Left*) Phase contrast and traction field maps of normal and tumor CE cells cultured on FN-coated flexible polyacrylamide gels for 4–6 h before measurement of cell traction. White arrows in traction maps indicate the direction of cell-generated traction forces on the underlying substrate; the color scale indicates the magnitude of traction (Pa). (*Right*) Quantitation of traction field maps using a previously described Matlab algorithm (47) showing the average ± SEM of maximum cumulative traction force (nN) exerted by individual CE cells ($n \geq 7$ per condition). (*B*) Tumor CE cells display higher baseline Rho activity than normal CE cells. Normal and tumor CE cells grown on FN-coated flexible silicone substrates were subjected to either no strain (Control) or 10% uniaxial cyclic strain (Strain) for 2 h, and Rho activity was analyzed by using the Rhotekin-RBD binding assay. (*Upper*) Representative western blot showing the levels of active GTP-Rho and total Rho for normal and tumor CE cells in the presence or absence of applied strain. (*Lower*) Relative changes in Rho activity under the various experimental conditions. GTP-Rho levels were measured as a percentage of total Rho levels and normalized to basal GTP-Rho levels in normal CE cells (**, $P < 0.002$ for comparison of baseline Rho levels in normal versus tumor CE cells). (*C*) ROCK activity in normal and tumor CE cells cultured under regular growth conditions, as determined by using a commercially available Rho-kinase assay. Bar graphs indicate the average OD450 value from triplicates.

they are more contractile than their normal counterparts are. To test this hypothesis directly, we analyzed normal and tumor CE cells by using traction force microscopy. Indeed, tumor CE cells exhibited large regions of stress concentration along their interface with the ECM substrate (Fig. 4*A*) and exerted nearly 2-fold greater traction forces than normal CE cells (Fig. 4*A*). Tumor CE cells also exhibited greater ECM adhesion strength and a slower rate of spreading despite similar levels of $\beta$1 and $\beta$3 integrin expression and activity (Fig. S4 and Fig. S5). Thus, the differential adhesion and spreading exhibited by tumor CE cells appears to arise from tension-dependent effects on focal adhesion assembly and cytoskeletal reorganization (27).

The small GTPase, Rho, regulates cytoskeletal tension generation and focal adhesion formation through its downstream effector, Rho-associated kinase (ROCK), which modulates myosin light chain phosphorylation (28). When cultured under normal growth conditions and subjected to Rhotekin pull down assays, tumor CE cells were found to exhibit an ≈2.5-fold higher level of baseline Rho activity than normal CE cells ($P < 0.001$) (Fig. 4*B*), which is consistent with their greater contractility (Fig. 4*A*). Tumor CE cells also exhibit abnormal Rho sensitivity to exogenous mechanical signals. When we applied 10% uniaxial cyclic strain for 2 h to normal and tumor CE cells cultured on flexible fibronectin (FN) substrates, the normal CE cells increased their Rho activity by ≈3-fold, whereas Rho activity remained unchanged in tumor CE cells (Fig. 4*B*). These data suggest that Rho was already optimally activated in these cells under baseline conditions. Moreover, the tumor CE cells also exhibited nearly 4-fold higher baseline ROCK activity than normal CE cells (Fig. 4*C*), which independently confirms that Rho is hyperactivated in these cells. Interestingly, levels of baseline Erk 1/2 activity were also 1.5-fold higher in tumor CE cells than in their normal counterparts (Fig. S6).

**Inhibition of ROCK-based Tension Restores Tumor CE Cell Mechanosensitivity.** The finding that Rho might be constitutively activated in tumor CE cells could explain why these cells fail to reorient normally in response to applied strain, because Rho signaling and cytoskeletal tension must decrease initially to produce this response (29). If this is true, then tumor CE cells might be able to be reprogrammed to behave like normal CE cells by artificially lowering their baseline level of cytoskeletal tension. To test this hypothesis, we pretreated tumor CE cells with the ROCK inhibitor, Y27632 (10 $\mu$M), for 30 min to reduce basal tension before exposure to cyclic strain. Under these conditions, a significantly greater percent of tumor CE cells (83% versus 60%; $P < 0.01$) realigned and reoriented their actin stress fibers perpendicular to strain direction (Fig. 5*A* and *B*). Decreasing basal cytoskeletal tension, however, produced the opposite effect in normal MDCE cells, with significantly fewer cells aligning with the direction of strain (Fig. 5 *A* and *B*; $P < 0.001$). More detailed analyses of the alignment response of individual cells within the different CE cell populations revealed that normal and tumor CE cells exhibit unique distribution profiles and that treatment with Y27632 restores a normal behavior distribution within the tumor CE cell population, whereas it disrupts this response in normal CE cells (Fig. S7). Furthermore, the same dose of Y27632 also rescued the tumor capillary collapse seen at the highest cell density and instead, promoted capillary network formation (Fig. 5*C*). In contrast, a similar reduction of tension in normal CE cells resulted in greater cell spreading and less tubular network formation (Fig. 5*C*). Therefore, these data suggest that differences between normal and tumor CE cell sensitivity to external mechanical forces and ECM compliance are governed by differences in the baseline levels of ROCK signaling and tension generation in these cells.

## Discussion

Past efforts aimed at dissecting the mechanisms underlying tumor vessel malformations showed that tumor-derived CE cells are distinct from those lining normal vessels at both the transcriptional and functional levels (30–32). These comparative

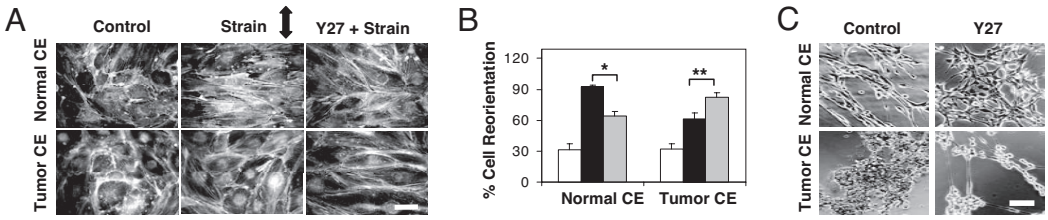


**Fig. 5.** Decreasing Rho-mediated tension significantly normalizes tumor CE behavior. (*A*) Inhibiting cell tension by pretreating CE cells with the ROCK inhibitor, Y27632, caused tumor CE cells to realign normally and reorient their actin stress fibers perpendicular to the applied strain direction, whereas it exerted an opposite effect on normal CE cells, as shown in the immunofluorescence micrographs. (Scale bar, 50 $\mu$m.) (*B*) Computerized morphometric quantitation of the reorientation response in cells (shown in *A*) cultured in the absence (Control, white bars) or presence of 10% uniaxial cyclic strain without (Strain, black bars) or with (Y27+Strain, gray bars) Y27632 pretreatment. Data are presented as the percentage of cells that reoriented 90° ± 30° relative to the direction of applied strain (*, $P < 0.01$; **, $P < 0.001$ for comparisons between strained samples treated with or without Y27632). (*C*) Phase contrast micrographs showing the opposing effects of Y27632-mediated reduction in cell tension on the angiogenic behavior of normal and tumor CE cells, when cultured on the surface of 3D fibrin gels. (Scale bar, 100 $\mu$m.)

studies, which focused solely on differences in canonical biochemical signaling pathways, revealed that tumor CE cells exhibit altered growth factor signaling arising from differential expression of important growth factor receptors (30, 32). Here, we show that tumor CE cells also exhibit aberrant Rho-mediated mechanosensitivity to physical cues from the ECM that are equally important for control of vascular development, and thus, these findings may have important implications for abnormal tumor angiogenesis.

In living tissues, CE cells are continuously exposed to flow-induced shear and cyclic strain forces that activate integrin-mediated mechanotransduction pathways and cause the cells to reorient their actin cytoskeleton parallel to blood flow and perpendicular to cyclic wall strain. Importantly, variations in hemodynamic forces can modify endothelial cell gene expression and function, which disrupts vascular homeostasis and promotes abnormal development (33). Abnormal hemodynamic forces resulting from turbulent blood flow and abnormal wall deformation in malformed tumor vessels could, therefore, alter CE cell behavior; however, it is also possible that these vascular malformations initially arise because CE cells lose their ability to sense and respond to normal mechanical cues, given that their neighboring cancer cells exhibit similar behavior (34). Therefore, in this study, we asked whether tumor CE cells exhibit aberrant responses to mechanical stimuli arising from ECM deformation and compliance.

Our *in vitro* studies revealed that tumor CE cells exhibit abnormal mechanosensitivity to uniaxial cyclic strain transmitted through the ECM, as seen by their failure to reorient perpendicularly to the strain direction. Endothelial cell reorientation in response to shear stress has previously been shown to be mediated by dynamic regulation of Rho activity, with the levels of GTP-Rho decreasing initially but increasing again within 1 h (29). These changes in Rho activity, which are similar to those observed during initial cell adhesion and spreading (35), likely reflect the need of adherent cells to first disassemble their preexisting focal adhesions and linked stress fibers to facilitate cell shape changes and cell reorientation before they can reassemble these structures and become stabilized in their newly aligned state. Indeed, increasing baseline Rho activity in endothelial cells by expressing constitutively active V14RhoA inhibits shear-induced cell reorientation (29).

Intriguingly, we found that, compared with normal CE cells, tumor CE cells failing to reorient in response to cyclic strain exhibit enhanced cytoskeletal tension as well as constitutively high baseline activities of Rho and ROCK, which appear to mediate the abnormal mechanosensitivity of tumor CE cells (34). Indeed, pretreatment with the ROCK inhibitor, Y27632, restored tumor CE cell reorientation in response to cyclic strain as well as capillary network formation at high cell plating densities. Additionally, whereas cyclic strain produced a ≈3-fold increase in GTP-Rho levels in normal CE cells, no apparent additional increase was observed in tumor CE cells. This finding implies that the constitutively high level of baseline Rho activity, rather than strain-induced Rho activation, prevents tumor CE cells from reorienting in response to cyclic strain.

Given that both normal and tumor CE cells express similar levels of active $\beta$1 and $\beta$3 integrins, our observations that tumor CE cells form thicker stress fibers, exert greater traction (contractility), display stronger adhesion strength, and spread more slowly than their normal counterparts appear to directly result from a higher intrinsic level of Rho and ROCK-dependent generation of cytoskeletal tension in these cells. These results explain why fewer tumor CE cells are required to exert the cumulative traction force on fibrin gels necessary for them to reorganize into capillary networks *in vitro*. It is also perhaps due to their enhanced contractility that tumor CE cells require stiffer substrates to achieve maximal shape stability (spreading), which occurs when cell traction forces are balanced by ECM resistance sites (14, 25).

The fact that tumor CE cells respond abnormally to the same mechanical environment that otherwise elicits physiological responses from normal CE cells suggests that CE cells may progressively acquire an altered phenotype as a result of being confronted by an abnormal mechanical and structural tumor microenvironment, much like the way epithelial tumor progression can be promoted by altering ECM structure or mechanics (34, 36–38). As a tumor grows, its stroma becomes stiffer than normal ECM, and the malignant epithelial cells exhibit higher Rho activity (39). Interestingly, in cultured breast epithelial cells, oncogenic transformation can also be stimulated by increasing either ECM stiffness or Rho-mediated tension, which feeds back to further increase ECM rigidity and hence, create a self-sustaining mechanical autocrine loop (34, 37).

Our findings suggest that, similar to transformed cancer cells, tumor CE cells likely adapt to the abnormal tumor physical environment by undergoing a reprogramming that involves enhanced Rho activation, increased tension generation, and possibly an autocrine mechanical feedback loop that sustains these effects to stabilize the aberrant phenotype. Circulating endothelial progenitor cells that are recruited in nascent vessels of certain tumors may also contribute to the abnormal tumor vessel structure and function through differentiation into actively dividing endothelial cells (40). Hence, they may also become deregulated by this abnormal mechanical environment.

Interestingly, we observed abnormal structural forms of 3D tumor capillaries *in vitro* that mimic the aberrant morphology

of tumor vessels seen *in vivo*. This could be due to our finding that tumor CE cells display a greater array of shapes over a larger range of ECM compliance compared with normal CE cells. Moreover, there might be an increased number of vessels because fewer tumor CE cells are required to form a capillary network and formation of a similar sized vessel with fewer cells would lead to more frequent intercellular gaps, as is observed in tumor vessels *in vivo* (41). In addition, the failure of tumor CE cells to reorient in response to cyclic wall strain may result in decreased packing of the endothelial monolayer and formation of structural discontinuities that could cause erratic blood flow, wall dilation, and increased vascular permeability. Leakage of plasma components and formation of perivascular fibrin gels can raise interstitial pressure and thus, ECM stiffness, which again may feed back to enhance Rho and ROCK activities in tumor CE cells and further promote their transformation into the stable abnormal phenotype we have observed in this study. Additionally, we found that tumor CE cell-conditioned medium partially inhibits normal CE cell mechanosensing (Fig. S8), whereas conditioned medium from normal CE cells has no detectable effect on tumor CE cells. This finding, combined with the observation that tumor CE cells have higher Erk 1/2 activity, suggests that soluble signals elicited by these cells may generate a positive feedback loop involving paracrine factors that serves to further deregulate the growth and form of normal CE cells in the cancer microenvironment, as has been observed during mechanical force-dependent stabilization of the oncogenic phenotype in breast cancer epithelial cells (34).

In conclusion, our results suggest that aberrant tumor microvasculature results from the inability of tumor CE cells to sense and respond normally to their physical microenvironment. This abnormal mechanosensitivity arises from higher Rho-mediated tension, which suppresses the ability of tumor CE cells to reorient in response to applied mechanical strain. Yet, at the same time, it enables these tumor CE cells to spread and form capillary networks over ECM material with a wide range of properties (stiffness), as compared with their normal counterparts. These differences in mechanosensitivity may explain why tumor microvessels exhibit much greater variability in shape and structural configuration than normal vessels, as well as why these vessels are dysfunctional. Further understanding of the role of the Rho signaling pathway and mechanotransduction in tumor vessel malformations may potentially lead to the development of novel vascular normalization and anti-cancer therapies in the future.

## Materials and Methods

**Cell Culture.** Tumor CE cells were isolated from transgenic TRAMP mice bearing prostate adenocarcinoma, as described elsewhere (42). Because it is difficult to obtain sufficient quantities of CE cells from the normal mouse prostate (due to its small size), we used normal CE cells isolated from the dermis (MDCE cells) of TRAMP mice. Normal CE cells from human dermis (HDCE cells; Cambrex) and an established mouse pancreatic CE cell line (43) (MS1-CE cells; gift of Judah Folkman) served as independent nontumor CE cell controls. Tumor CE cells, MDCE, and MS1-CE cells were cultured on FN-coated tissue culture dishes and grown in culture medium composed of low glucose DMEM, 10% FBS, 10% Nu Serum IV, basic fibroblast growth factor (6 ng/ml), heparin salt (0.1 mg/ml), 1% insulin-transferrin-selenium, and an antibiotic/mycotic mixture. These cells were used between passages 10–19. HDCE cells were grown on tissue culture dishes in medium as per manufacturer's protocol and used between passages 4–8.

**Mechanical Strain Application.** CE cells were cultured on FN-coated, flexible silicone substrates (Uniflex plates, Flex Cell International) to ≈70–80% confluence and then exposed to 10% uinaxial cyclic strain (1 Hz) for 18 h using a Flexercell Tension Plus System (Flex Cell International), as previously described (44). Cells cultured on the same substrates in the same incubator but not receiving applied strain were treated as controls. In some experiments, cells were pretreated with the ROCK inhibitor, Y27632 (10 $\mu$M, 30 min), rinsed, and supplemented with fresh medium before application of cyclic strain.

**Modulation of ECM Elasticity.** Transglutaminase-cross-linked gelatin hydrogels of increasing stiffness were prepared with a final gelatin concentration of 3, 5, or 10% (wt/vol) and incubated at 37°C overnight to stabilize cross-linking, as previously described (45). Stiffness measurements were performed by using an AR-G2 rheometer (TA Instruments) with a standard aluminum parallel plate geometry of 20 mm. Hydrogels were subjected to a stress sweep (46), and their storage moduli (G′) were compared under the same physical conditions. To analyze the effects of varying ECM elasticity on cell shape, we cultured CE cells for 6 h on hydrogels of varying stiffness at a low density (1,000 cells per squared centimeter) to minimize cell–cell interactions.

***In Vitro* Angiogenesis Assay.** Capillary network formation by CE cells was analyzed by using a two-dimensional fibrin gel assay, which was modified from a previously described fibrin-based *in vitro* assay (47). Thrombin-cross-linked fibrin gels (3 mg/ml) were formed in 48-well plates and incubated at 37°C for 30 min before normal and tumor CE cells were plated in culture medium at densities of 2, 3, 4, or $8 \times 10^4$ cells per well. Cells were cultured at 37°C for 24 h before tube formation was analyzed. In some experiments, cells plated at the highest density ($8 \times 10^4$ cells per well) and cultured for 3 h were treated with Y27632 (10 $\mu$M), and capillary network formation was monitored after 24 h. To analyze capillary organization by CE cells cultured within (as opposed to on top of) 3D ECM gels, we resuspended normal or tumor CE cells at a high density ($5 \times 10^6$ cells per milliliter) in either fibrin gel (5 mg/ml) or Matrigel and cultured the cells in regular growth medium for 1 day or 2 wk, respectively.

**Analysis of Cellular Traction Forces.** Traction forces exerted by CE cells on their ECM adhesions were measured by using traction force microscopy. Cells were grown on thin (≈100 $\mu$m), FN-coated, flexible polyacrylamide gels (Young's modulus = 14 kPa) containing fluorescent nanobeads (100 nm diameter) as fiduciary markers, as previously described (48).

**Rho Activation Assay.** Rho activity was determined by using the Rhotekin-RBD binding assay (Cytoskeleton), as described elsewhere (35). Cells grown on FN-coated flexible silicone substrates with or without 10% uniaxial cyclic strain for 2 h were lysed in RIPA buffer, and equal volumes of clarified lysate were treated with GST-Rhotekin-RBD beads for 1 h at 4°C. The beads were pelleted, washed, and treated with SDS-sample buffer to solubilize bead-bound GTP-Rho, which was detected by using western blot analysis. Baseline ROCK activity in normal and tumor CE cells cultured under regular growth conditions was measured by using a commercially available Cyclex Rho-kinase Assay Kit-384 (MBL International, MA), as per manufacturer's protocol.

**Microscopy, Image Analysis, and Statistics.** Images of live cells forming tubular structures in the *in vitro* angiogenesis assay and of cells cultured on compliant gelatin hydrogels fixed with 4% paraformaldehyde were recorded by using a Nikon Diaphot 300 phase contrast microscope (Nikon) fitted with a Hamamatsu digital camera (Hamamatsu Photonics). In other studies, cells were fixed with 4% paraformaldehyde, permeabilized with 0.2% Triton X-100, stained with Alexa Fluor-488 Phalloidin and DAPI (to visualize actin and nuclei, respectively), and imaged by using an Nikon Eclipse TE 2000-E microscope (Nikon) fitted with a CoolSnap HQ digital camera (Photometrics). Image analyses were performed by using ImageJ software (National Institutes of Health). For cyclic strain experiments, computerized morphometric analysis of fluorescence images was carried out to determine the angle between the longest axis of the cell and the direction of applied cyclic strain; these results are reported as the percentage of cells aligned at 90° ± 30° relative to the direction of the applied strain.

For cell spreading studies, projected cell areas were measured by tracing cell perimeters, and the areas were normalized to their respective mean values from the earliest time point or the most compliant substrate. For densitometric analyses of western blots, levels of GTP-Rho were expressed as a percentage of total Rho levels, and then normalized to baseline (control) GTP-Rho levels in normal CE cells. All data were obtained from multiple replica experiments and are expressed as mean ± SEM. Statistical significance was determined by using Student's unpaired *t* test (InStat; GraphPad).

For more information, please see *SI Text*.

**ACKNOWLEDGMENTS.** We thank Dr. Harold Dvorak for helpful discussions. This work was supported by National Institutes of Health grants CA-45548 (to D.E.I. and M.K.), CA-58833 (to D.E.I.), and CA-37392 (to M.K.). D.E.I. is a recipient of a Department of Defense Breast Cancer Innovator Award.

1. Dvorak HF (2003) Rous-Whipple Award Lecture. How tumors make bad blood vessels and stroma. *Am J Pathol* 162:1747–1757.
2. Baluk P, Hashizume H, McDonald DM (2005) Cellular abnormalities of blood vessels as targets in cancer. *Curr Opin Genet Dev* 15:102–111.
3. Jain RK (1998) The next frontier of molecular medicine: Delivery of therapeutics. *Nat Med* 4:655–657.
4. Jain RK (2001) Normalizing tumor vasculature with anti-angiogenic therapy: A new paradigm for combination therapy. *Nat Med* 7:987–989.
5. Lee CG, *et al.* (2000) Anti-Vascular endothelial growth factor treatment augments tumor radiation response under normoxic or hypoxic conditions. *Cancer Res* 60:5565–5570.
6. Dickson PV, *et al.* (2007) Bevacizumab-induced transient remodeling of the vasculature in neuroblastoma xenografts results in improved delivery and efficacy of systemically administered chemotherapy. *Clin Cancer Res* 13:3942–3950.
7. Nagy JA, Dvorak AM, Dvorak HF (2007) VEGF-A and the Induction of Pathological Angiogenesis. *Annu Rev Pathol* 2:251–275.
8. Winkler F, *et al.* (2004) Kinetics of vascular normalization by VEGFR2 blockade governs brain tumor response to radiation: Role of oxygenation, angiopoietin-1, and matrix metalloproteinases. *Cancer Cell* 6:553–563.
9. Dike LE, *et al.* (1999) Geometric control of switching between growth, apoptosis, and differentiation during angiogenesis using micropatterned substrates. *In Vitro Cell Dev Biol Anim* 35:441–448.
10. Ingber DE, Folkman J (1989) Mechanochemical switching between growth and differentiation during fibroblast growth factor-stimulated angiogenesis in vitro: Role of extracellular matrix. *J Cell Biol* 109:317–330.
11. Matsumoto T, *et al.* (2007) Mechanical strain regulates endothelial cell patterning in vitro. *Tissue Eng* 13:207–217.
12. Davis GE, Senger DR (2005) Endothelial extracellular matrix: Biosynthesis, remodeling, and functions during vascular morphogenesis and neovessel stabilization. *Circ Res* 97:1093–1107.
13. Korff T, Augustin HG (1999) Tensional forces in fibrillar extracellular matrices control directional capillary sprouting. *J Cell Sci* 112(Pt 19):3249–3258.
14. Kumar S, *et al.* (2006) Viscoelastic retraction of single living stress fibers and its impact on cell shape, cytoskeletal organization, and extracellular matrix mechanics. *Biophys J* 90:3762–3773.
15. Ghosh K, *et al.* (2007) Cell adaptation to a physiologically relevant ECM mimic with different viscoelastic properties. *Biomaterials* 28:671–679.
16. Ingber DE (2003) Tensegrity II. How structural networks influence cellular information processing networks. *J Cell Sci* 116:1397–1408.
17. Huang S, Ingber DE (1999) The structural and mechanical complexity of cell-growth control. *Nat Cell Biol* 1:E131–138.
18. Padera TP, *et al.* (2004) Pathology: Cancer cells compress intratumour vessels. *Nature* 427:695.
19. Paszek MJ, Weaver VM (2004) The tension mounts: Mechanics meets morphogenesis and malignancy. *J Mammary Gland Biol Neoplasia* 9:325–342.
20. Yasuhara K, Kimura K, Nakamura H, Uchibori T, Hirama M (1997) New color Doppler technique for detecting turbulent tumor blood flow: A possible aid to hepatocellular carcinoma diagnosis. *J Clin Ultrasound* 25:183–188.
21. Bershadsky AD, Balaban NQ, Geiger B (2003) Adhesion-dependent cell mechanosensitivity. *Annu Rev Cell Dev Biol* 19:677–695.
22. Ingber D (1991) Integrins as mechanochemical transducers. *Curr Opin Cell Biol* 3:841–848.
23. Iba T, Sumpio BE (1991) Morphological response of human endothelial cells subjected to cyclic strain in vitro. *Microvasc Res* 42:245–254.
24. Kaunas R, Nguyen P, Usami S, Chien S (2005) Cooperative effects of Rho and mechanical stretch on stress fiber organization. *Proc Natl Acad Sci USA* 102:15895–15900.
25. Chicurel ME, Chen CS, Ingber DE (1998) Cellular control lies in the balance of forces. *Curr Opin Cell Biol* 10:232–239.
26. Dvorak HF (1986) Tumors: Wounds that do not heal. Similarities between tumor stroma generation and wound healing. *N Engl J Med* 315:1650–1659.
27. Burridge K, Wennerberg K (2004) Rho and Rac take center stage. *Cell* 116:167–179.
28. Kimura K, *et al.* (1996) Regulation of myosin phosphatase by Rho and Rho-associated kinase (Rho-kinase). *Science* 273:245–248.
29. Tzima E, del Pozo MA, Shattil SJ, Chien S, Schwartz MA (2001) Activation of integrins in endothelial cells by fluid shear stress mediates Rho-dependent cytoskeletal alignment. *EMBO J* 20:4639–4647.
30. Bussolati B, Deambrosis I, Russo S, Deregibus MC, Camussi G (2003) Altered angiogenesis and survival in human tumor-derived endothelial cells. *FASEB J* 17:1159–1161.
31. St Croix B, *et al.* (2000) Genes expressed in human tumor endothelium. *Science* 289:1197–1202.
32. Amin DN, Hida K, Bielenberg DR, Klagsbrun M (2006) Tumor endothelial cells express epidermal growth factor receptor (EGFR) but not ErbB3 and are responsive to EGF and to EGFR kinase inhibitors. *Cancer Res* 66:2173–2180.
33. Gimbrone MA, Jr, Topper JN, Nagel T, Anderson KR, Garcia-Cardena G (2000) Endothelial dysfunction, hemodynamic forces, and atherogenesis. *Ann N Y Acad Sci* 902:230–240.
34. Paszek MJ, *et al.* (2005) Tensional homeostasis and the malignant phenotype. *Cancer Cell* 8:241–254.
35. Ren XD, Kiosses WB, Schwartz MA (1999) Regulation of the small GTP-binding protein Rho by cell adhesion and the cytoskeleton. *EMBO J* 18:578–585.
36. Ingber DE, Madri JA, Jamieson JD (1981) Role of basal lamina in neoplastic disorganization of tissue architecture. *Proc Natl Acad Sci USA* 78:3901–3905.
37. Huang S, Ingber DE (2005) Cell tension, matrix mechanics, and cancer development. *Cancer Cell* 8:175–176.
38. Sympson CJ, Bissell MJ, Werb Z (1995) Mammary gland tumor formation in transgenic mice overexpressing stromelysin-1. *Semin Cancer Biol* 6:159–163.
39. Fritz G, Just I, Kaina B (1999) Rho GTPases are over-expressed in human tumors. *Int J Cancer* 81:682–687.
40. Nolan DJ, *et al.* (2007) Bone marrow-derived endothelial progenitor cells are a major determinant of nascent tumor neovascularization. *Genes Dev* 21:1546–1558.
41. Hashizume H, *et al.* (2000) Openings between defective endothelial cells explain tumor vessel leakiness. *Am J Pathol* 156:1363–1380.
42. Dudley AC, *et al.* (2008) Calcification of multipotent, prostate tumor endothelium. *Cancer Cell*, in press.
43. Arbiser JL, *et al.* (1997) Oncogenic H-ras stimulates tumor angiogenesis by two distinct pathways. *Proc Natl Acad Sci USA* 94:861–866.
44. Kumar A, Murphy R, Robinson P, Wei L, Boriek AM (2004) Cyclic mechanical strain inhibits skeletal myogenesis through activation of focal adhesion kinase, Rac-1 GTPase, and NF-kappaB transcription factor. *FASEB J* 18:1524–1535.
45. Yung CW, *et al.* (2007) Transglutaminase crosslinked gelatin as a tissue engineering scaffold. *J Biomed Mater Res A* 83:1039–1046.
46. Ghosh K, *et al.* (2005) Rheological characterization of in situ cross-linkable hyaluronan hydrogels. *Biomacromolecules* 6:2857–2865.
47. Nicosia RF, Ottinetti A (1990) Modulation of microvascular growth and morphogenesis by reconstituted basement membrane gel in three-dimensional cultures of rat aorta: A comparative study of angiogenesis in matrigel, collagen, fibrin, and plasma clot. *In Vitro Cell Dev Biol* 26:119–128.
48. Tolic-Norrelykke IM, Butler JP, Chen J, Wang N (2002) Spatial and temporal traction response in human airway smooth muscle cells. *Am J Physiol Cell Physiol* 283:C1254–1266.